16th World Conference on Earthquake Engineering, 16WCEE 2017

Santiago Chile, January 9th to 13th 2017

Paper N° 3395(Abstract ID)

Registration Code: S-XXXXXXXX

SEISMIC FRAGILITY EXAMINATION OF SIMPLY SUPPORTED CURVED PRESTRESSED CONCRETE BRIDGE PORTFOLIOS

J. Seo[(1)], LP. Rogers[(2)]

[(1)] *Assistant Professor, Department of Civil and Environmental Engineering South Dakota State University, SD 57007, USA, junwon.seo@sdstate.edu*
[(2)] *Bridge E.I.T., HDR, 701 Xenia Avenue South, Suite 600, Minneapolis, MN, USA, luke.rogers@hdrinc.com.*

Abstract

This paper examines the seismic vulnerability of single-span, simply supported, curved, prestressed concrete (PSC) I-girder bridge portfolios with various characteristics using fundamental fragility concepts that have been commonly used. Experimental design technique was used as a statistical means of comparison between varying bridge configurations, ultimately producing a wide variety of hypothetical PSC I-girder bridges. Structural design of each bridge was made according to the guidelines specified by the AASHTO LRFD Bridge Design Specifications. To examine seismic vulnerability to seismic excitations, non-linear time history analyses (NLTHAs) was conducted using multiple synthetic ground motions. Response of critical components was extracted for fragility analysis and comparison. Fragility curves were created via probabilistic seismic demand models (PSDM) following established techniques. The preliminary fragility data were analyzed to determine the effects of the varying design parameters on seismic vulnerability of the bridge portfolios. The results found that the shorter span bridges with a tighter radius of curvature are less sensitive to seismic excitations than those with straighter decking.

Keywords: Curved Bridges, Prestressed Concrete I-Girders, Seismic Analysis, Vulnerability, Sensitivity, Ground Motions

1. Introduction

Bridges can be considered a critical link during natural disasters such as seismic events and the importance of their functionality during such events is of critical interest to the community as a whole. Bridges using straight prestressed concrete (PSC) I-girders with curved decking which are capable of fulfilling the ever growing needs of today's national transportation system have been built in locations around the county, including seismically active regions. Many studies have attempted to establish the risk of failure during seismic events using fragility analysis [1-5], while none have examined the seismic fragility of simply supported, curved PSC I-girder bridges. Hence, this study examines the seismic vulnerability of 15 simply supported, curved PSC I-girder bridge portfolios with various characteristics. Design parameters, such as span length, deck width, curvature, and column configuration were determined and entered into an experimental design technique to generate the varying bridge configurations. Bridges were then modeled using a 3D finite element program which subjected each bridge to 30 different ground motion time histories. The ground motions included two horizontal acceleration components and one vertical acceleration component to mimic real world conditions with varying intensities. Investigation of the results will determine the effect of two-span bridge configurations and design parameters such as curvature, span length, width, number of spans, and column configuration on bridge fragility in terms of peak ground accelerations (PGAs).

2. Curved PSC Bridge Portfolios

To create various hypothetical PSC I-girder bridges, utilizing an experimental design method was valid [4-5, 6]. The program JMP (SAS, 2000) was employed to allow the Central Composite Design (CCD) technique to generate the bridge portfolios. Again, bridges were categorized as single span, simply-supported curved PSC I-girder bridges. Classing was required to simplify experimental design, increase analysis efficiency, and allow for distinct recognition of parameter effects. Parameters used for the bridge class included span length, deck width, and deck offset enabling to create radius of curvature.

To produce the CCD-based bridge portfolios, three levels of each parameter, including a lower, middle, and upper level were employed. Table 1 provides the selected parameters used for the CCD-based bridge portfolios. Upon completion of the CCD bridge inventory, the result was a set of 15 single-span bridges with different configurations. Bridge design for single-span bridges followed the procedures and characteristics outlined in past study [7].

Table 1. Key design parameters with three CCD levels for PSC bridges.

	Single Span		
	Lower	Middle	Upper
Span Length (m)	21.3	33.5	48.7
Offset (m)	0.15	0.30	0.45
Deck Width (m)	9.1	12.2	18.3

3. 3D Computational Modeling

To model each of the bridges, a three-dimensional finite element program was utilized to accurately represent the structural and material nonlinearities. The bridge components exhibit highly nonlinear behavior during an earthquake so it is desirable to use nonlinear finite element analysis in a 3D setting to better represent actual conditions during seismic excitations. To accomplish this, the program CSiBridge was used for both bridge design checks and seismic analysis. Each bridge is made up of various modeling elements, such as frames and springs. A representative curved PSC bridge schematic and details along with its elevation view can be seen in Figure 1. The representative bridge is single span, simply supported, with a 21 m span length utilizing four AASHTO Type III I-Girders. The width is 9 m and the offset is 0.46 m creating a radius of curvature equal to 123 m. The seat type abutment uses eight piles.

Piles were represented by trilinear springs which have an effective stiffness of 7 kN/mm/pile and vertical stiffness was taken as 175 kN/mm/pile as reported by Choi et al. [1]. Abutments were modeled using beam-frame elements consisting of appropriate cross sections and material properties representing the seat-type abutment and concrete of 27 MPa. Passive earth pressure on the abutment backwall was modeled using quadralinear springs developed by Nielson and DesRoches [2] with varying effective stiffness depending on abutment dimensions. Generally, the initial stiffness of the passive pressure was approximately 23 kN/mm per one meter of width. Next, bearings were modeled using bilinear plastic springs. Bearings in this bridge type consisted of elastomeric pads and embedded steel dowels to prevent horizontal shifting of the girder. Elastomeric pad stiffness depended on dimensions of the pad and shear modulus, therefore the stiffness varied between bridge models. Using a shear modulus of 200 MPa, the effective stiffness of the pads was approximately 6 kN/mm per pad. Two steel dowels were used per bearing with an effective stiffness of 92 kN/mm [1]. Stiffness for the vertical axis on the bearing allowed for free movement upward and limited movement below the initial position. To model this, a gap element was used which provides support but simulates no upward restraint and allows the superstructure to lift-off from the bearing and abutment. In this way, actual conditions were replicated where the self-weight of the superstructure is the only significant resistance to vertical separation of the girder and the support.

The effect of impact was modeled using multi-linear springs to simulate the collision of the superstructure with the abutment backwall during seismic events. A 75 mm expansion joint separates the abutment from the superstructure and impact occurs when this gap closes and the spring is activated. Stiffness for these springs was determined using formulas from past research [2]. The spine modeling technique was implemented to represent the finite element 3D bridge models. In this technique all bridge girders, deck sections, and diaphragms were modeled using a single frame element with the appropriate cross section and spacing for the superstructure components used in design. Concrete compressive strength of the girders was 48 MPa and 27 MPa for the decking. Tendons were modeled using frame elements representing the Grade 270, 7-wire strand. Tendon prestress force was 1100 MPa after all losses including concrete creep, shrinkage, tendon relaxation, and tendon elastic shortening.

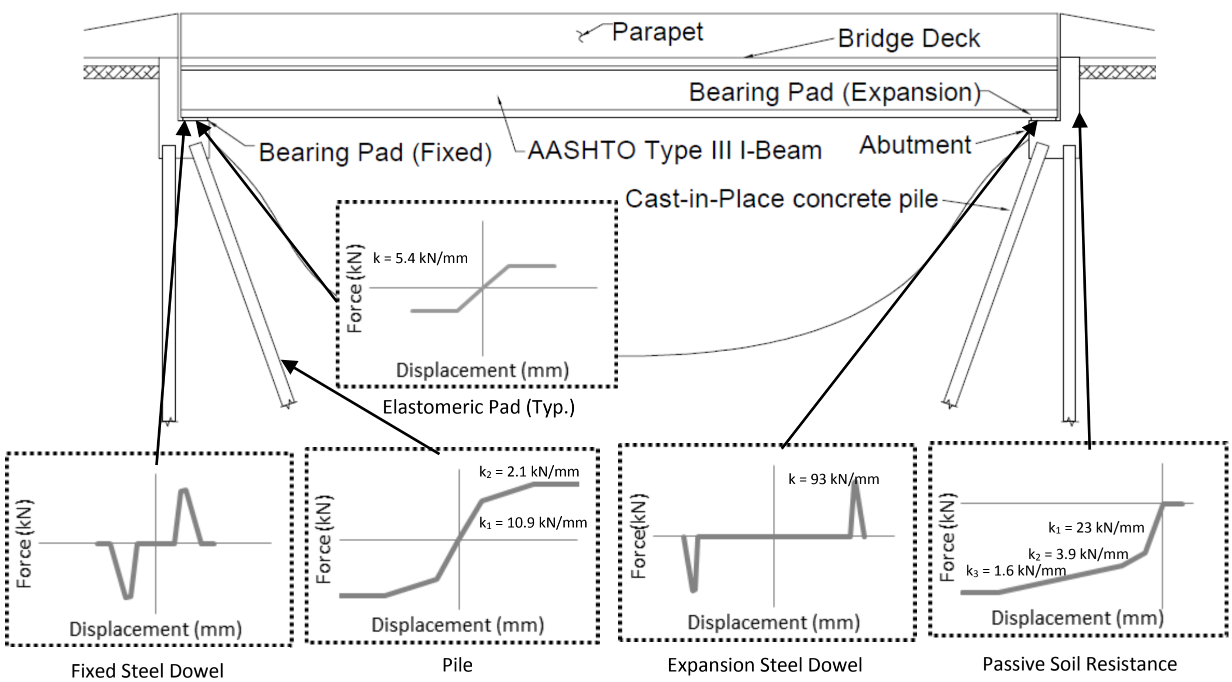

Fig. 1 – 3D simply supported PSC bridge model

4. Ground Motions

Synthetic ground motions were acquired from the University of New York at Buffalo [8]. These ground motions were selected based on the desire to have a variable range of PGAs and the fact that ground motion time histories from earthquakes in the central United States are not readily available. A total of 30 ground motions with PGA values ranging from 0.10g to 1.10g were applied to the base of the abutment in each model. These ground motions contained acceleration time histories in all three orthogonal directions, including longitudinal, transverse, and vertical directions. Figure 2 shows selected spectral accelerations. Due to model complexity and computer limitations, the vertical ground accelerations were applied separately from the horizontal ground accelerations. During the vertical acceleration-based simulations, the effect of gravity must be considered; thus, the acceleration of gravity was applied simultaneously to simulate the effects of dead load on bridge components during the seismic events.

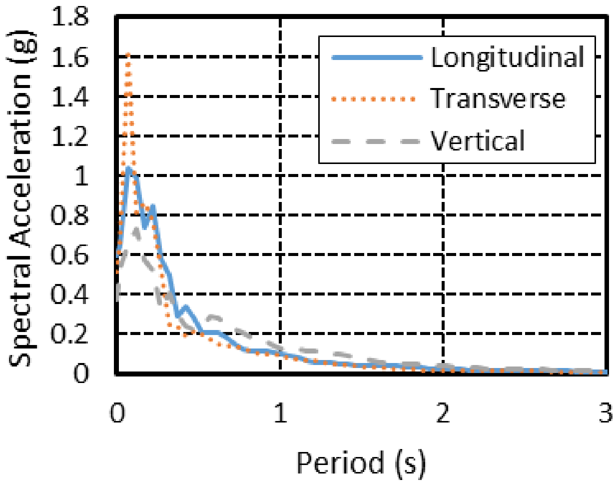

Fig. 2 – Selected spectral accelerations for all three orthogonal directions

5. Fragility Analysis

5.1 Limit States

To create fragility curves, quantitative limit states must be defined for a particular damage state. Limits states can be defined using either the prescriptive or descriptive approaches. The prescriptive approach is where an analyst prescribes the functional level of the bridge based on the physics of the system, while the descriptive approach is to describe the limits that bridge officials would place on a bridge if they observed various levels of damage [9]. The prescriptive limit states for horizontal bridge behaviors have been defined by [9] and the relevant descriptive limits were found by [10] who conducted a survey to obtain them. These limit states were then integrated using the Bayesian theory. These updated values for horizontal excitations were used in this study for damage limit states as shown in Table 2. Prescriptive limit states for vertical bridge behaviors were established by Wang et al. [11] for investigating the effects of vertical ground motions on bridge-foundation systems. However, these limits were defined in a way that did not correlate well for use in this study since the limits defined damage in the horizontal direction due to vertical ground motions. Hence, simplified limits were used based upon the strength and/or serviceability limits according to the AASHTO specifications. The strength limit for the piles was defined as the compressive strength of the concrete and steel reinforcing. This limit remains constant since the pile diameter is 0.40 m for all the bridges. The compressive stress limit for bearing pads was taken from the AASHTO specifications which specify a stress limit of 5.5MPa for plain elastomeric pads [12]. The serviceability limit for deflections of the midspan of all the bridges was conservatively taken as span/1000 from the AASHTO Specifications [12].

Table 2. Limit states.

Orientation	Component	Slight	Moderate	Extensive	Complete/ Design Limit (Vertical only)
Horizontal	Elastomeric Bearing -Long (mm)†	28.9	104.2	136.1	186.6
	Elastomeric Bearing -Tran (mm)†	28.8	90.9	142.2	195
	Abutment Trans/Long(mm)†	9.8	37.9	77.2	100
	Columns (μ_φ) (curvature ductility)	1	1.64	3.43	7.4
Vertical	Elastomeric Bearing (kPa)*	NA	NA	NA	5,500
	Abutment Piles (kN)	NA	NA	NA	3,660
	Midspan (mm)*	NA	NA	NA	Span/1000

Note:
† indicates the limit states are taken from Nielson [9]
* Indicates the limit states are taken from the AASHTO Specifications [12]

5.2 Fragility Curve Generation

Fragility curves are created using the analytical method where a broad range of ground motions are applied to bridge models to capture seismic responses of each of their critical components. From these responses, a probabilistic seismic demand model (PSDM) is generated by linear regression analysis of the response data. A limit predetermined at a damage state is assigned to each component and fragility curves in the form of PSDM can be generated following Equation 1.

$$P_f = \Phi\left(\frac{ln\left(\frac{S_D}{S_C}\right)}{\sqrt{\beta_d^2+\beta_c^2}}\right) \tag{1}$$

where P_f is the exceedance probability, S_c is the median value of the structural capacity defined for the damage state, β_c is the dispersion or lognormal standard deviation of the structural capacity, S_d is the calculated seismic demand in terms of a chosen ground motion intensity parameter, β_d is the logarithmic standard deviation for the demand and Φ is the standard normal distribution function. Further details on the standard fragility curve generation can be found in the work of Choi et al. [1] and Seo et al. [12].

5.3 Component-Level Fragility Curves

Using the aforementioned limit states and standard fragility equations, seismic fragility curves for each component of all 15 bridges were created. These included abutments and bearings. Again, all three orthogonal directions were taken into consideration for the component-level fragility analysis. The component fragility curves are shown in Figure 3 as an example for the representative bridge (see Figure 1). It can be seen that the most fragile component is the abutment in the transverse direction. The next most fragile component is the bearing in the longitudinal direction. Both the expansion and fixed type bearing have identical fragility, the median PGA is estimated at about 2.0g in the longitudinal direction. This results from the fact that the movement of the expansion bearing is dependent of the movement of the fixed bearing and they share the same limit states [1, 9]. For the bearing in the transverse direction, the median PGA is very high and insignificant. The trend occurring in Figure 3(b;d) shows that the probability of exceeding median PGA is unlikely for the horizontal directions at higher damage states.

In addition to the exploration of horizontal bridge movement fragility, the vertical fragility of components are included in Figure 3(d) for the design limit state. It appears that the bearing has the most likelihood of damage by exceeding the serviceability limits. Midspan deflection resulting from vertical excitations was monitored, and the probability of exceeding the serviceability limit state is also shown in Figure 3(d).

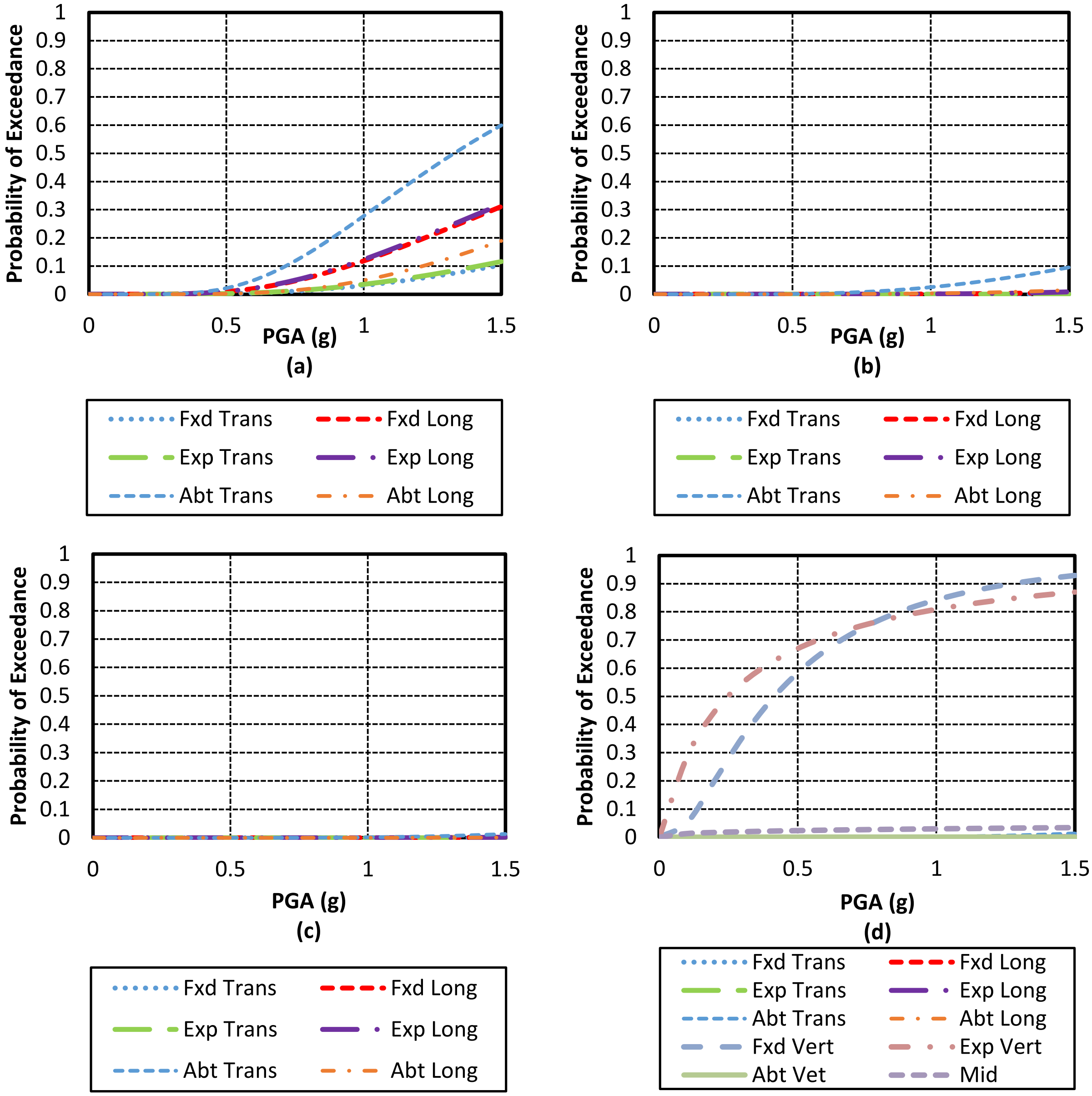

Fig. 3 – Component fragilities for representative single span bridge: a) slight damage, b) moderate damage, c) extensive damage, and d) complete damage (includes vertical component fragility).

5.4 System Fragility Curves

To investigate vulnerability sensitivity, a system level fragility curve is required for each bridge. To accomplish this, the probability of exceedance of bridge components can be joined via the following equation, resulting in a fragility curve for a bridge system.

$$max_{i=1}^{m}[P(F_i)] \leq P(F_{sys}) \leq \prod_{i=1}^{m}[1-P(F_i)] \quad (2)$$

where $P(F_{sys})$ is the cumulative probability, $P(F_i)$ is the component probabilities. This procedure for the system level fragility curve generation is further detailed in past work [1, 9]. Figure 4 illustrates the system level fragility curves for the representative bridge. It can be seen in Figure 4(a) for horizontal ground motions that the median PGA for the slight damage state is about 0.9g. For the moderate, extensive, and complete damage states, the corresponding median PGA is very high and therefore insignificant. These results indicate that the probability of slight damage, such as concrete spalling or cracking, is possible during a seismic event. Conversely, it is shown that for the complete damage state, which represents structural failure of the bridge, damage is unlikely to occur. As illustrated in Figure 4(b), the median PGA is approximately 1.75g for system fragility resulting from vertical ground motions. Therefore, during seismic events with high PGA values, the bridge is moderately fragile in the vertical direction.

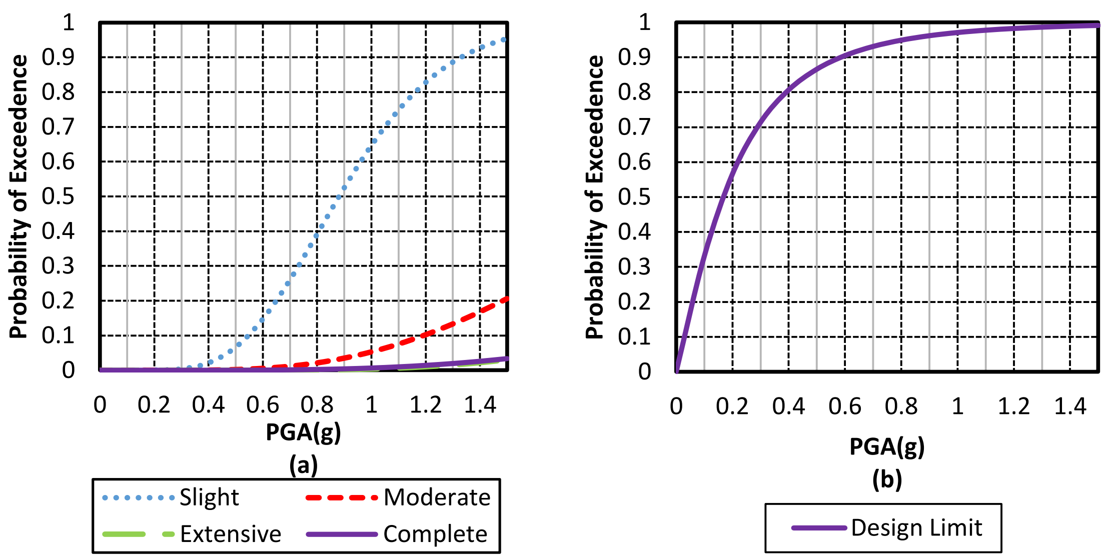

Fig. 4 – System level fragility curves for a represetrative single span bridge: a) horizontal ground motions and b) vertical ground motions.

6. Effects of Design Parameters

To determine the effect of S/R ratio on system fragilities for the curved PSC bridges, the value of the remaining parameter, width, was fixed and bridge fragilities were grouped accordingly based on that bridge width. Average probabilities of the bridge fragilities were used for comparison. As an example for the slight damage state, there are three fragility curves for the 9 m wide bridges as shown in Figure 5(a), one for each S/R ratio used. This figure indicates that the median PGA for the bridges with the S/R ratio less than 0.05 is 0.60g for slight damage, while the least fragile are those bridges with S/R ratios greater than 0.10 where the median PGA is approximately 0.90g. This is a percent difference of nearly 41%. This trend continues to the wider bridges where the percent difference between most and least fragile S/R ratios is roughly 31% and 22% for the 12 m and 18 m bridges, respectively, for the slight damage state. This trend continues for the remaining damage states. It can be seen in Figure 5(b) that the trend is for the bridges with a lower S/R ratio to exhibit more fragility. This is due to the fact that a longer bridge will have a greater superstructure mass which typically increases the likelihood of damage to components during seismic events.

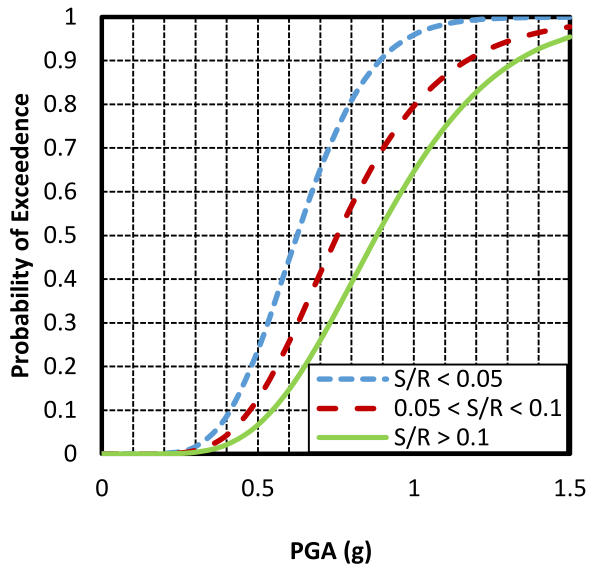

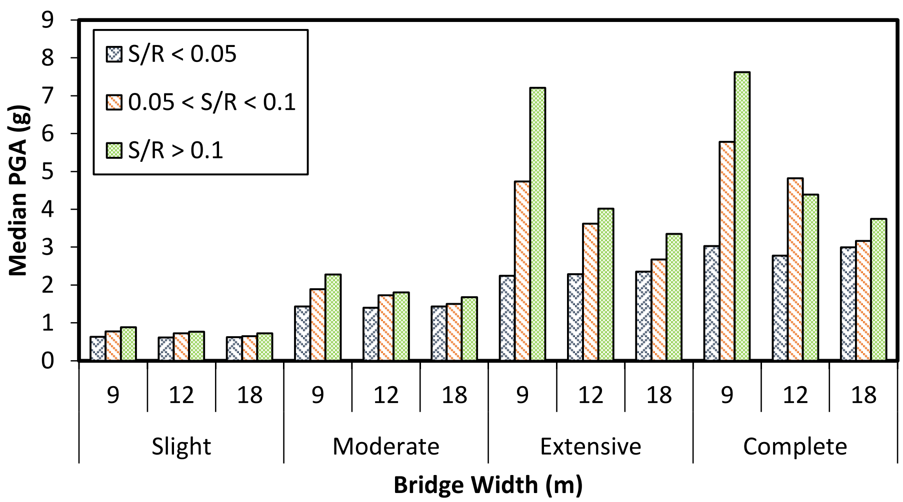

Fig. 5 – S/R ratio effect on bridge fragility: a) representative curves for 9m wide bridges for the slight damage state and b) median PGA values for each damage state.

To examine the effect of bridge width on the bridge fragilities, the bridges with similar S/R ratios but varying widths were compared. Figure 6(a) shows the slight damage fragility curves for the sample bridges with S/R ratio between 0.05 and 0.10. Figure 6(b) shows multiple bar charts for median PGAs of the bridges with different S/R ratios. This figure indicates that the most fragile bridges, under slight damage, have a median PGA of about 0.60g and the least fragile ones have a median of nearly 0.75g. This is a difference of approximately 22%. The trend in the slight damage largely continues for the rest of damage states. Overall, the results indicate that wider bridges demonstrate more fragile behaviors. This can be attributed to increased superstructure mass. A wider bridge typically places more load on each bearing due to greater girder spacing, therefore a larger bearing is required. This in turn results in a higher bearing stiffness, although it can be concluded that this increase in stiffness was not sufficient enough to reduce seismic responses of wider bridges in this study.

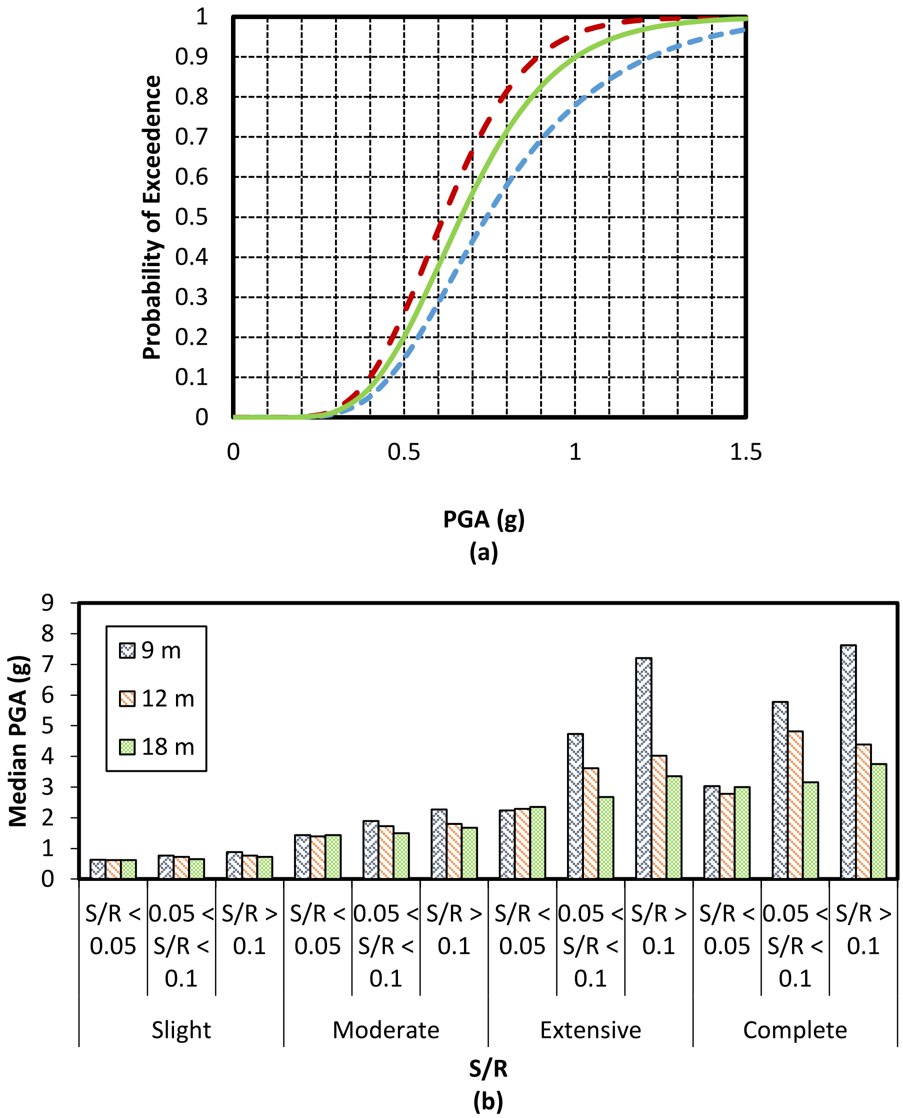

Fig. 6 – Effect of deck width on bridge fragility: a) Slight damage state representative fragility curves for S/R between 0.05 and 0.10 and b) median PGAs for each damage state.

7. Conclusions

This paper examined the seismic vulnerability sensitivity of single-span, simply-supported curved prestressed concrete (PSC) I-girder bridges. The experimental design utilized the Central Composite Design (CCD) technique to create a wide variety of hypothetical bridges based on selected design parameters, including span length, offset, and deck width. A non-linear time history analysis (NLTHA) using synthetic ground motions was conducted to establish seismic demands on critical bridge components. Damage states were obtained from past research for the horizontal directions. Vertical limit states did not exist in a usable form for this study, and therefore the states were established using the strength and service design limits for the components of interest. Using probabilistic seismic demand models (PSDMs) and established fragility functions, component and system level fragility curves were generated to explore the seismic vulnerability of the bridges. Further, the effects of the design parameters on the seismic vulnerability were examined, and the span length to radius of curvature (S/R) ratio and bridge width were used to facilitate efficient comparison in the seismic vulnerability between bridges.

System-level fragility of the bridges under ground motions was investigated to determine the seismic vulnerability sensitivity. The design for the bridge type showed that a tighter radius of curvature requires a shorter span, whereas a larger radius of curvature utilized longer spans. As a result of this configuration, it was found that a low S/R ratio would exhibit less fragility than a bridge with a higher S/R ratio. It was also demonstrated that increasing the width of a bridge unfavorably affected the system fragility. As the deck width increases, the fragility increased due to the larger superstructure mass and for increased load per bearing for the single-span bridges.

8. Acknowledgements

The authors acknowledge partial financial support from the Scholarly Excellence Funds Program at South Dakota State University.

9. References

[1] Choi, E., DesRoches, R., Nielson, B. (2004). “Seismic fragility of typical bridges in moderate seismic zones.” Eng. Struct. 26(2), 187–99.

[2] Nielson, B., and DesRoches, R. (2006). “Influence of modeling assumptions on the seismic response of multi-span simply supported steel girder bridges in moderate seismic zones.” Eng. Struct., 28(8), 1083–1092.

[3] Padgett, J. and DesRoches, R. (2008). “Methodology for the development of analytical fragility curves for retrofitted bridges.” Ethqk. Eng. and Struct. Dyn., 37(8), 1157-1174.

[4] Seo, J. and Linzell, D. (2012). “Horizontally curved steel bridge seismic vulnerability assessment.” Eng. Struct., 34, 21-32.

[5] Seo, J. and Linzell, D. (2013). “Use of response surface metamodels to generate system level fragilities for existing curved steel bridges.” Eng. Struct., 52, 642-653.

[6] Simpson, T. W., Peplinski, J. D., Koch, P. N., and Allen, J. K. (2001). “Metamodels for Computer-Based Engineering Design: Survey and Recommendations,” Eng. with Computers, 17(2), 129-150.

[7] Rogers, L. P., (2015). “A Compilation of Research on Seismic Vulnerability of Curved Concrete bridges using Straight Precast I-Girders.” Masters Thesis. South Dakota State University. Brookings South Dakota.

[8] Engineering Seismology Laboratory. (2005). SUNY at Buffalo. Buffalo, New York. http://civil.eng.buffalo.edu/engseislab/index.htm. Accessed March 2014.

[9] Nielson, B. (2005). “Analytical Fragility Curves for Highway Bridges in Moderate Seismic Zones.” Ph.D. thesis, School of Civil and Environmental Engineering, Georgia Institute of Technology, Atlanta, Georgia.

[10] Padgett, J. (2007). “Seismic Vulnerability Assessment of Retrofitted Bridges Using Probabilistic Methods.” Ph.D. thesis, Georgia Institute of Technology, Atlanta.

[11] Wang, Z., Padgett, J.E., Duenas-Osorio, L. (2013). “Influence of vertical ground motions on the seismic fragility modeling of a bridge-soil-foundation system”. *Earthq. Spectra*, 29(3), 987-962.

[12] AASHTO. (2012). LRFD Bridge Design Specifications. Washington DC.

[13] Seo, J., Dueñas-Osorio, L., Craig, JI, and Goodno, BJ (2013). “Metamodel-based regional vulnerability estimate of irregular steel moment-frame structures subjected to earthquake events.” Engineering Structures 45, 585-597.